Local orientational order in ice

Frank H. Stillinger and Martha A. Cotter*
Bell Laboratories, Murray Hill, New Jersey 07974
(Received 9 October 1972)

A cluster expansion approach for the Kirkwood orientational correlation factor g_K in ice has been examined. The expansion parameter measures the extent to which neighboring molecules obey bonding requirements of the "ice rules." For cubic ice, leading terms have been evaluated in the series for the separate contributions to g_K from the first three shells of neighbors. These series tend to confirm the validity of a recent Monte Carlo estimate of g_K, but they also suggest that orientational order in cubic and hexagonal ices has long range and is analogous to local order of critical point pair correlations in Ising models. As a result, the cluster expansion for g_K itself likely converges very slowly, if at all.

I. INTRODUCTION

The Kirkwood theory of polar dielectrics[1] establishes the intimate connection between intermolecular forces, and static dielectric response. The corresponding Kirkwood formula, in the absence of polarizability, relates the zero-frequency dielectric constant ϵ_0 to the mean-square molecular dipole moment $\langle\mu^2\rangle$ as follows:

$$(\epsilon_0-1)(2\epsilon_0+1)/\epsilon_0=4\pi\rho\langle\mu^2\rangle g_K/kT. \qquad (1.1)$$

Here ρ stands for the molecular number density, k is Boltzmann's constant, and T is the absolute temperature.

The explicit influence of the intermolecular forces enters this formula through the Kirkwood orientational correlation factor g_K, which reflects the extent to which hindered rotation of neighboring molecules tends to align their dipole directions. The prescription by which g_K is to be calculated places a typical molecule (numbered 1) at the center of a region ω with large size on the molecular scale, but still comprising a vanishing fraction of the entire system volume V. In precise terms,

$$g_K=\lim_{\omega\to\infty}\{\lim_{V\to\infty}\langle\sum_{j\text{in}\omega}\boldsymbol{\mu}_1\cdot\boldsymbol{\mu}_j\rangle/\langle\mu^2\rangle\}, \qquad (1.2)$$

where $\boldsymbol{\mu}_i$ denotes the dipole moment vector for molecule i.

The double limit shown in Eq. (1.2) is basic, as Kirkwood himself clearly stated. Long-range dipole–dipole interactions (whose influence may be assessed with the aid of macroscopic electrostatics[1]) create long-range orientational correlations which are weak for any widely separated pair of molecules, but which produce nonnegligible effects when summed over the full system. Thus the alternative quantity

$$G_K=\lim_{V\to\infty}\langle\sum_{j\text{in}V}\boldsymbol{\mu}_1\cdot\boldsymbol{\mu}_j\rangle/\langle\mu^2\rangle \qquad (1.3)$$

will not in general equal g_K. For polar fluid dielectrics one has[1]

$$G_K=[9\epsilon_0/(\epsilon_0+2)(2\epsilon_0+1)]g_K. \qquad (1.4)$$

The evaluation of g_K in polar liquids presents a formidable challenge to statistical mechanics, due in part to the diverse local structural arrangements exhibited by molecules in liquids. It is therefore especially attractive to consider the less demanding task of calculating g_K in solids with known crystal structure. We have elected specifically to investigate the cubic modification of ice, "ice Ic."

Both cubic ice Ic, and its more familiar hexagonal form ice Ih, consist of three-dimensional hydrogen-bond networks, with ubiquitous fourfold tetrahedral coordination.[2] The oxygen atoms form the termini of the hydrogen bonds, and the protons are distributed among the bonds according to the Bernal–Fowler ice rules[3]:

(1) One and only one proton resides along each bond.
(2) Two equilibrium positions are available to each proton along its bond, depending on the oxygen to which it is covalently attached.
(3) Precisely two protons are covalently bound to each oxygen (i.e., the crystal consists of intact water molecules).

In spite of the stringency of the ice rules,[4] substantial freedom remains in the way the water molecules rotate into coincidence with the tetrahedral bond directions. Under the assumption that all of the canonical Bernal–Fowler ice structures have nearly the same energy, Pauling[5] quantitatively explained the residual entropy of ice as a direct manifestation of water molecule orientational degeneracy.

The ice model for which we attempt to evaluate g_K is logically identical to Pauling's; namely, equal *a priori* weights accorded to all canonical Bernal–Fowler arrangements. We furthermore suppose that the individual molecular dipole moments are identical in magnitude from one canonical structure to the next.

A two-dimensional analog of real ice proves to be an easy and convenient means for visualizing various aspects of the proton disorder phenomenon. Figure 1 shows an 8×8 portion of two-dimensional "square ice" which, like its three-dimensional relatives, has fourfold coordination, and six possible molecular configurations at each site. The latter attribute is attained however at the expense of including zero-dipole-moment configurations, in which the water molecules are linear.

Owing to the discrete structures of the two and three-dimensional ices, the Kirkwood factor g_K for these models may be expressed as a sum over separate

neighbor types:

$$g_K=1+\sum_{\nu=1}^{\infty} m_\nu \frac{\langle \mu_1\cdot\mu_{j(\nu)}\rangle_\infty}{\langle \mu^2\rangle}. \tag{1.5}$$

The correlation of molecule 1 with itself provides the leading term unity; the number of νth type neighbors [a typical one of which is denoted by $j(\nu)$] has been symbolized by m_ν. To be consistent with the ordered double limit specified in Eq. (1.2), the infinite-system (subscript ∞) dipole correlation functions are required for the summand in Eq. (1.5).

There have been several other attempts to evaluate g_K for one or more of the ices. Powles[6] concluded that $g_K\cong 2.65$ for ice Ih, by examining small clusters of molecules excised from the extended crystal. Hollins,[7] on the other hand, observed that systematic neglect of hydrogen-bond ring closures (logically related to Pauling's combinatorial approximation[5]) in an infinite crystal would require $g_K=3$ for both Ic and Ih structures; he furthermore estimated that ring closures should modify this simple result by no more than one percent.

More recently, Gobush and Hoeve[8] have adapted the existing cluster expansion techniques for the ice problem[9–11] to direct calculation of g_K. This method yields an infinite series for g_K, which they carried out explicitly through twelfth order:

$$\begin{aligned} g_K=1&+4(1/3)+4(1/3)^2+4(1/3)^3+4(1/3)^4+4(1/3)^5\\ &-4(1/3)^6-12(1/3)^7+36(1/3)^8+84(1/3)^9\\ &+132(1/3)^{10}+292(1/3)^{11}+748(1/3)^{12}+\cdots. \end{aligned} \tag{1.6}$$

Under the seemingly plausible assumption that succeeding terms are numerically negligible, this gives 2.99584. Thus Hollins' conclusion that ring closures are unimportant might at first glance appear to be supported.

The square ice model shown in Fig. 1, and a related set of two-dimensional ferroelectrics, have themselves been the object of intense theoretical study.[12–17] There exists a real possibility that the methods which permit exact evaluation of the partition functions for these models could be adapted to calculation of the individual quantities $\langle \mu_1\cdot\mu_j\rangle_\infty$ appearing in Eq. (1.5). Subsequently the corresponding g_K could be obtained.

In general, the potential energy for an icelike lattice model can be written as follows (neglecting molecular polarization):

$$\Phi(1,\cdots,N)-\mathbf{E}\cdot\sum_{i=1}^{N}\boldsymbol{\mu}_i; \tag{1.7}$$

the first term represents intermolecular interactions, and the second couples the dipoles to an external homogeneous electric field E. By insisting that periodic boundary conditions apply, these models become spatially homogeneous. If the linear dielectric response to E is isotropic (i.e., if the system has square symmetry in two dimensions, or cubic symmetry in three dimensions), then it is straightforward to show that the leading field dependence of the free energy F is

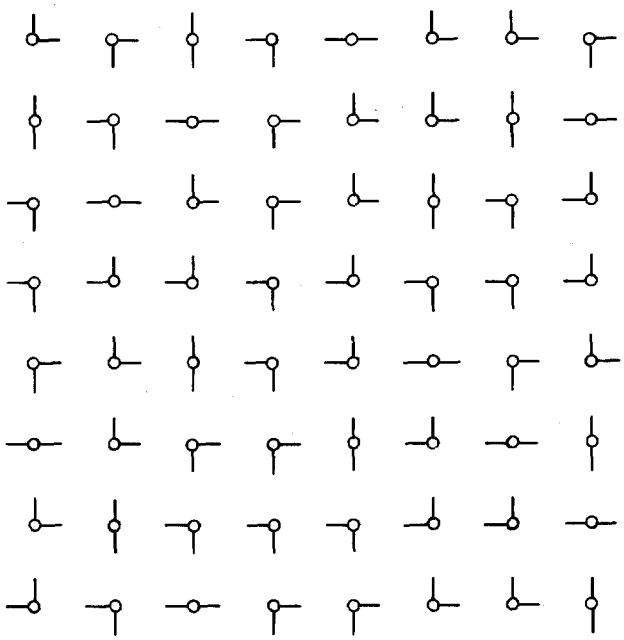

FIG. 1. Canonical configuration for an 8×8 sample of square ice. Periodic boundary conditions have been imposed. Covalent OH bonds are denoted by solid lines.

$$F(\mathbf{E})=F(0)-N\langle \mu^2\rangle G_K E^2/2kT, \tag{1.8}$$

in which G_K, the quantity already introduced by Eq. (1.3), may be written in the alternative form[18]:

$$G_K=1+\sum_{j=2}^{N}[\langle \mu_1\cdot\mu_j\rangle/\langle \mu^2\rangle]. \tag{1.9}$$

We have already noted that long-range dipole–dipole forces produce a distinction between g_K and G_K. But even if these forces are absent, the ice rules themselves manage to induce a comparable distinction. The source of this effect is obvious in the case of square ice shown in Fig. 1. The total number of OH molecular groups pointing horizontally to the right is the same for all vertical rows of molecules. In other words, the horizontal component of the total moment must be identical for all columns. A similar comment applies to the total vertical moment of every horizontal row in Fig. 1.

One expects the total system moment

$$\mathbf{M}=\sum_{i=1}^{N}\boldsymbol{\mu}_i \tag{1.10}$$

to fluctuate, with a mean-square magnitude proportional to N,

$$\langle M^2\rangle=NG_K\langle \mu^2\rangle, \tag{1.11}$$

for both two- and three-dimensional cases. The horizontal (x) component of a total column moment, $m_x=M_x/N^{1/2}$ for a square sample of square ice, then has a mean-square magnitude independent of N; i.e., it has order unity. The statistical bias conferred on the x

component of an arbitrary molecular moment, say μ_1, when its column has fixed $m_z \cong 1$, will be proportional to $N^{-1/2}$. On account of the rigid interlocking of successive columns, another widely separated dipole μ_j will at the same time be forced to display a similar x component bias proportional to $N^{-1/2}$. Thus at very large separations in square ice,

$$\langle \mu_{1x} \mu_{jx} \rangle = C/N, \tag{1.12}$$

where the coherence of column moment fluctuations requires

$$C > 0. \tag{1.13}$$

Including both moment directions, we therefore write for large separations[19]

$$\langle \boldsymbol{\mu}_1 \cdot \boldsymbol{\mu}_j \rangle = C'/N, \quad C' > 0. \tag{1.14}$$

An exactly analogous situation arises for the three-dimensional ice models. The polarization handed along through the crystal from one puckered hexagonal layer to the next, projected along the direction normal to those layers, must be constant. The mean-square moment fluctuation per layer is now proportional to $N^{1/3}$, but the typical bias per molecule will be proportional to $N^{-1/2}$ as before since there are on the order of $N^{2/3}$ molecules per layer. Consequently, Eq. (1.14) also describes the situation in three dimensions, as well as in two.

By definition, G_K receives a positive contribution from the long-ranged, weak correlation between dipoles that results from the rigid ice rules, which g_K does not contain. In contrast to the relation (1.4) which refers to polar fluids, we now have the ice-model inequality

$$G_K > g_K. \tag{1.15}$$

Nagle[20] has recently devised a cluster expansion technique whereby the field-dependent free energy $F(\mathbf{E})$, shown in Eq. (1.8), can be directly evaluated. By use of a clever graph-vertex renormalization that varies with the applied field, Nagle is able to eliminate a wide class of cluster graphs from his analysis, thereby minimizing computational effort. The conclusion is that $G_K = 3.002$ for ice Ic, and for the dielectric response of ice Ih along its c axis the value 3.005 obtains. Nagle also points out that G_K for square ice in two dimensions can be extracted from the existing exact solutions for the free energy of two-dimensional ferroelectric models,[14,16] and that his cluster expansion appears to agree well with that result.

An independent source of information about orientational order in ice is provided by the ability to construct small crystallites in accordance with the ice rules, using a rapid electronic computer. Rahman and Stillinger[21] have carried out such an investigation for samples of both ice Ic (4096 molecules) and ice Ih (2048 molecules). The Monte Carlo procedure employed generates many (but far from all) representative Bernal–Fowler configurations with equal *a priori* weights. By averaging over the canonical structures generated, it was possible to obtain not only g_K, but also its separate coordination shell contributions. Evaluation of the distinct quantity G_K however was not feasible with the specific approach selected.

The Monte Carlo results for ice Ic indicated that

$$g_K = 2.11 \pm 0.10; \tag{1.16}$$

for ice Ih a small anisotropy appeared, but averaging over directions results in a very similar number

$$g_K = 2.07 \pm 0.02. \tag{1.17}$$

By comparison with Hollins' estimate, and with the Gobush–Hoeve calculation, these Monte Carlo results seem anomalously low. They are however consistent with Nagle's prediction, in the light of inequality (1.15). One of our major goals in this paper will be clarification of these numerical disparities.

Section II introduces and explains the formal perturbation expansion with which we calculate the individual pair correlations $\langle \boldsymbol{\mu}_1 \cdot \boldsymbol{\mu}_j \rangle_\infty$. This approach is very closely related to that of Gobush and Hoeve,[8] but we offer it here in a rather different mathematical setting.

Section III provides details of our specific cluster series coefficient evaluations. Considerable effort has been expended on the first- and second-coordination shell correlations. The results agree with the Monte Carlo calculations, and thus provide partial verification of that approach. The results also indicate that for ice the perturbation theory must be evaluated at its singular limit of convergence. The delicate mathematical situation, to put it in other terms, arises from the fact that ice corresponds roughly to an Ising model at its critical point, and incorporates correlations that are probably not exponentially damped with increasing distance.

Our final section, Sec. IV, points out directions for potentially fruitful further research on ice models.

II. PERTURBATION EXPANSION

It has been traditional[9–11] to represent the six distinct water molecule orientations at site i of the crystal by a state parameter ξ_i,

$$1 \leq \xi_i \leq 6. \tag{2.1}$$

If ξ_i and ξ_j are the orientation state parameters for two sites that are connected by a bond (that is, i and j are nearest-neighbor sites), then the ice rules strictly forbid occurrence of 18 out of the 36 possible pairs (ξ_i, ξ_j). These forbidden pairs of course are those which lead either to zero or two protons along the bond (i.e., Bjerrum defects).

The most convenient mathematical setting for our analysis results from temporary relaxation of the ice rules. Thus we shall assign to each nearest-neighbor

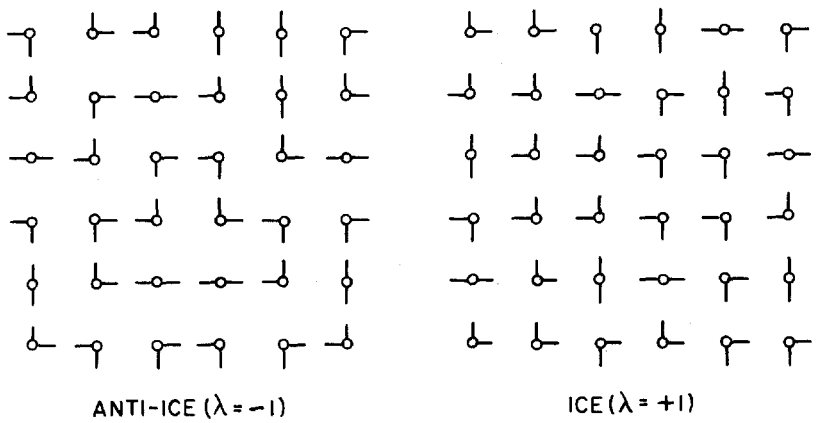

FIG. 2. Conjugate ice and anti-ice configurations for a 6×6 square ice system. Interconversion results from reversing the configuration of every other molecule.

pair an energy $\pm w$:

$$+w \text{ (0 or 2 protons along bond)},$$
$$-w \text{ (1 proton along bond)}. \quad (2.2)$$

By requiring w eventually to approach $+\infty$, the conventionally disallowed (ξ_i, ξ_j) pairs will naturally disappear.

In accord with the energy assignment (2.2), we define the following bond function ($\beta = 1/kT$):

$$B[\xi_i, \xi_j] = \exp(-\beta w)/[\exp(\beta w)+\exp(-\beta w)] \quad \text{(0 or 2 protons along bond)},$$
$$= \exp(\beta w)/[\exp(\beta w)+\exp(-\beta w)] \quad \text{(1 proton along bond)}. \quad (2.3)$$

The product of such B's for all $2N$ bonds in the crystal forms a suitable weighting function for the problem in hand:

$$F(\xi_1 \cdots \xi_N) = \prod_{b=1}^{2N} B_b[\xi_{l(b)}, \xi_{u(b)}]; \quad (2.4)$$

here and in the following we shall employ periodic boundary conditions. In this expression for F the index b refers to an arbitrary numbering of the bonds; the crystal however has been oriented so that each bond has identifiable lower (l) and upper (u) ends.

In the limit $w \to \infty$, the factors B have values 0 or 1, and so F becomes unity for all configurations satisfying the ice rules, but vanishes for those which do not. Again in that limit, the number of distinct canonical ice configurations (Bernal–Fowler structures) is provided by the quantity

$$W_N = \sum_{\xi_1=1}^{6} \cdots \sum_{\xi_N=1}^{6} F(\xi_1 \cdots \xi_N). \quad (2.5)$$

Averages over the canonical structures may be calculated with the weight F, and for the specific quantities required for the Kirkwood factor g_K one has

$$\langle \boldsymbol{\mu}_1 \cdot \boldsymbol{\mu}_j \rangle = (W_N)^{-1} \sum_{\xi_1=1}^{6} \cdots \sum_{\xi_N=1}^{6} \boldsymbol{\mu}_1(\xi_1) \cdot \boldsymbol{\mu}_j(\xi_j) F(\xi_1 \cdots \xi_N). \quad (2.6)$$

To be consistent with Eq. (1.2), we shall use this expression only in the infinite system limit, $N \to \infty$.

Next set

$$\lambda = \tanh(\beta w), \quad (2.7)$$

so that the bond function B_b has the simple representation

$$B_b[\xi_i, \xi_j] = \tfrac{1}{2}\{1+\lambda a_b[\xi_i, \xi_j]\}. \quad (2.8)$$

Here $a_b[\xi_i, \xi_j]$ is $+1$ if the pair of orientations is compatible with the ice rules, and -1 otherwise. The quantity λ will be the basic perturbation parameter of our treatment, and we shall seek to provide power series expansions both for W_N and for the $\langle \boldsymbol{\mu}_1 \cdot \boldsymbol{\mu}_j \rangle$ in this "coupling constant." It is appropriate to call λ an "orientational hindrance parameter," since as it increases from zero ($w=0$) to unity ($w=+\infty$), molecules in the crystal pass from a condition of arbitrary $\xi_1 \cdots \xi_N$ choice to complete adherence to the ice rules.

Although we are ultimately obliged to set $\lambda = +1$,[22] it will be informative along the way to inquire about the behavior of the several functions of interest throughout the complex λ plane. A special significance attaches to the point $\lambda = -1$ in this plane, which corresponds to the limit $w \to -\infty$. In this limit, every bond in the crystal is forced to display a Bjerrum defect, to produce a sort of "anti-ice" that everywhere violates the ice rules.

Every closed polygon in the ice crystals (Ih, Ic, or the square ice model) has an even number of sides. As a result the sites may be partitioned into two sublattices, with members of one sublattice serving as nearest neighbors to members of the other sublattice. By reversing[23] the configuration of every water molecule on one of the sublattices, a valid ice configuration is uniquely converted to an anti-ice configuration, and vice versa. The numbers of canonical configurations for ice and for anti-ice are therefore equal,

$$W_N(-1) = W_N(+1). \quad (2.9)$$

Figure 2 displays a pair of conjugate configurations for ice and for anti-ice, in the square ice model. Notice that pairs of covalent OH bonds oppose one another in the latter. The dipole moment of each molecule may

consistently be regarded as the vector sum of two parts, directed respectively along the OH covalent bonds. In a crystal satisfying periodic boundary conditions, and having precisely equal numbers of molecules on the two sublattices, the total moment $\mathbf{M}$ of the system vanishes exactly.[24] Equation (1.11) in the preceding section allows us to conclude that

$$G_K(-1)=0. \tag{2.10}$$

Owing to the fact that its zero moment does not fluctuate, anti-ice can have no dipole orientation contribution to its dielectric constant ϵ_0. In the absence of polarization effects, ϵ_0 for anti-ice would therefore be unity, and Kirkwood's formula (1.1) implies that

$$g_K(-1)=0. \tag{2.11}$$

The same conclusion can be reached from Eq. (2.10) supplemented by realization that long-range contributions which cause G_K to exceed g_K in ice are subject to wholesale cancellation after the sublattice reversal operation. Equation (2.11) provides a useful fixed point against which to check theoretical calculations.

The λ expansion for $W_N(\lambda)$ may be initiated by inserting form (2.8) for B_b into Eq. (2.5).

$$W_N(\lambda)=2^{-2N}\sum_{\xi_1=1}^{6}\cdots\sum_{\xi_N=1}^{6}\prod_{b=1}^{2N}\{1+\lambda a_b[\xi_{l(b)},\xi_{u(b)}]\}$$
$$=(3/2)^N\sum_{\xi_1=1}^{6}\cdots\sum_{\xi_N=1}^{6}6^{-N}\prod_{b=1}^{2N}\{1+\lambda a_b[\xi_{l(b)},\xi_{u(b)}]\}. \tag{2.12}$$

Square ice has two types of neighbor bonds b (horizontal and vertical), and therefore two distinct functions a_b. The bonds in cubic ice are of four geometric types, and seven geometric types occur in hexagonal ice. Nagle[11] has shown that for all three models and bond types, the functions a_b may be factored:

$$a_b(\xi_i,\xi_j)=-C_{ij}(\xi_i)C_{ji}(\xi_j). \tag{2.13}$$

The quantity $C_{ij}(\xi_i)$ is $+1$ if configuration ξ_i places a proton of molecule i along the ij bond, -1 otherwise. Similarly $C_{ji}(\xi_j)$ is $+1$ or -1 according to whether or not molecule j has a proton along the same bond. Thus

$$W_N(\lambda)=(3/2)^N\sum_{\xi_1\cdots\xi_N}6^{-N}\prod_{\text{bonds}}\{1-\lambda C_{ij}(\xi_i)C_{ji}(\xi_j)\}. \tag{2.14}$$

When expression (2.14), a polynomial in λ of degree $2N$, is put into fully expanded form, the individual terms may be placed into correspondence with linear graphs drawn on the model's basic lattice. The lines of the graphs connect neighboring vertices, and indicate the presence of the pair $C_{ij}C_{ji}$ in the corresponding term. The coefficient of λ^n is composed out of all terms (graphs) with exactly n $C_{ij}C_{ji}$ pairs (lines).

The special advantage of Nagle's factorization, Eq. (2.13), is the ease with which it allows one to show that many terms in the expansion of W_N vanish. It can thus be established[10,11] that the only surviving terms are those whose graphs contain solely vertices of even order; i.e., each lattice vertex has zero, two, or four lines impinging upon it. The weight associated with a given graph then will be [before including the common factor $(3/2)^N$]

$$\lambda^n/3^{p_2}, \tag{2.15}$$

where p_2 is the number of order-two vertices in the n-line graph.

Similar considerations apply to the individual λ-dependent dipole correlation quantities (i and j here are a pair of type ν, where $\nu=1$ means nearest neighbors, etc.):

$$\Gamma^{(\nu)}(\lambda)\equiv\langle\boldsymbol{\mu}_i\cdot\boldsymbol{\mu}_j\rangle_\lambda/\langle\mu^2\rangle$$
$$=\Big[\sum_{\xi_1\cdots\xi_N}6^{-N}\boldsymbol{\mu}_i(\xi_i)\cdot\boldsymbol{\mu}_j(\xi_j)\prod_{\text{bonds}}\{1-\lambda C_{ij}(\xi_i)C_{ji}(\xi_j)\}\Big]/|\boldsymbol{\mu}|^2\sum_{\xi_1\cdots\xi_N}6^{-N}\prod_{\text{bonds}}\{1-\lambda C_{ij}(\xi_i)C_{ji}(\xi_j)\}. \tag{2.16}$$

The denominator here is the same expression [aside from the factor $(3/2)^N$] shown for $W_N(\lambda)$, and the preceding graphical prescription applies to it. The numerator differs only by the special status conferred on vertices i and j by the presence of $\boldsymbol{\mu}_i\cdot\boldsymbol{\mu}_j$; the numerator graphs must have even vertices everywhere *except* for i and j, which must be odd (one or three incident lines). The weight appropriate to each such n-line numerator graph was shown by Gobush and Hoeve[8] to be

$$-(\lambda^n/3^{p_2+1})\,\mathbf{u}_i\cdot\mathbf{u}_j, \tag{2.17}$$

where $\mathbf{u}_i$ and $\mathbf{u}_j$ are unit vectors for the respective sites, with directions determined by the vector sum of graph lines leaving those sites.

We shall use these graphical criteria in the next section to evaluate coefficients of leading terms in the W_N and $\Gamma^{(\nu)}$ power series for cubic ice.

III. SERIES COEFFICIENT EVALUATION

On account of the restrictions which apply to its graphs, W_N receives its first cluster contributions from isolated hexagons; i.e., the contributions are sixth order in λ. In orders λ^8 and λ^{10}, respectively, it is necessary to enumerate the corresponding isolated octagons and decagons. For the cubic ice lattice under consideration, these enumerations are simple.

Complications begin to arise at order λ^{12}. Of course isolated dodecagons (there are seven distinct types for ice Ic) contribute, but so also do graphs with two independent hexagons, as well as those "figure-eight" graphs consisting of two hexagons with a shared vertex.

The 14th order proved to be the practical limit in the present work on W_N. In this order it was necessary to catalog the 35 distinct tetrakaidecagons (14-sided polygons), to find the number of distinguishable ways to place an octagon and a hexagon on the lattice without overlapping, and to count graphs consisting of a vertex-sharing octagon–hexagon pair.

The final result for large N is found to be

$$W_N(\lambda)=(3/2)^N\{1+2N(\lambda/3)^6+3N(\lambda/3)^8 +24N(\lambda/3)^{10}+(2N^2+165N)(\lambda/3)^{12} +(6N^2+870N)(\lambda/3)^{14}+\cdots\}. \quad (3.1)$$

Since only even orders in λ appear, consistency with Eq. (2.9) is assured. The highest power of N to occur in the coefficient of a given λ order equals the maximum number of disconnected parts possible with graphs of that order. Thus we expect N^3 to occur first in the λ^{18} coefficient (3 hexagons), N^4 to occur first with λ^{24} (4 hexagons), etc.

It is more informative to exhibit W_N as an Nth power. The required Nth root of the series in Eq. (3.1) is easy to construct, and leads to the following expression:

$$W_N(\lambda)=\{(3/2)[1+2(\lambda/3)^6+3(\lambda/3)^8+24(\lambda/3)^{10} +167(\lambda/3)^{12}+876(\lambda/3)^{14}+\cdots]\}^N. \quad (3.2)$$

The separate terms beyond unity in the correction factor to Pauling's $\frac{3}{2}$ are quite small for $\lambda=\pm1$, and are declining with increasing order. If it is legitimate merely to truncate the series at fourteenth order, one obtains

$$W_N(\pm1)\cong\{1.506157\}^N. \quad (3.3)$$

Nagle's earlier calculation of W_N[10] was similar to that just outlined, but without benefit of a natural ordering parameter such as λ. Consequently he grouped graphs according to ascending number of second-order vertices (rather than number of sides), and concluded from his 14th-order calculation

$$W_N(1)\cong\{1.50685\pm0.00015\}^N. \quad (3.4)$$

The two estimates (3.3) and (3.4) resoundingly affirm the excellence of Pauling's approximation. It is possible that Eqs. (3.3) and (3.4) could be brought into even closer agreement with one another if Padé approximant analysis[25] were brought to bear on the series (3.2), but in the absence of further information on location and nature of singularities in the complex λ plane, this elaboration seems unwarranted.

We turn next to the nearest-neighbor correlation function $\Gamma^{(1)}(\lambda)$. Graphs generated by the numerator of expression (2.16) will always have an odd number of lines for nearest neighbors, so their contribution to $\Gamma^{(1)}$ will be odd in λ. As we have seen in calculation of $W_N(\lambda)$, the denominator involves only even orders in λ, so in fact $\Gamma^{(1)}(\lambda)$ will be an odd function of λ, and in particular

$$\Gamma^{(1)}(-1)=-\Gamma^{(1)}(+1). \quad (3.5)$$

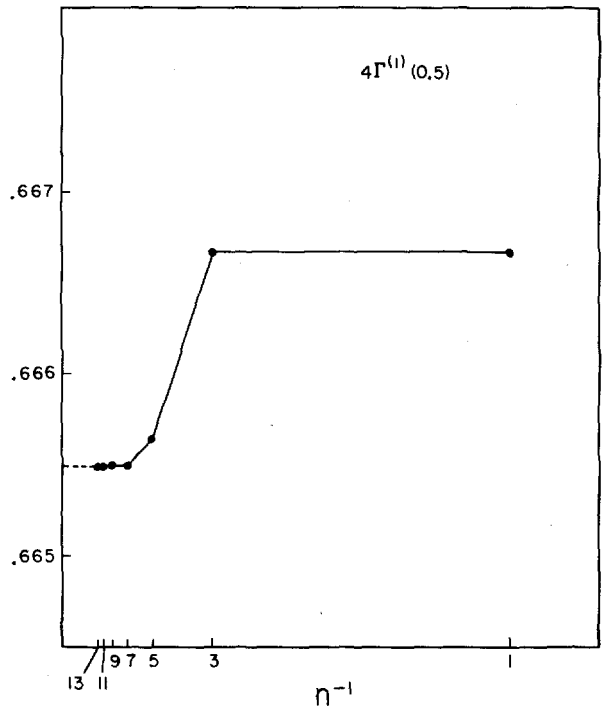

FIG. 3. Partial sums for $4\Gamma^{(1)}(0.5)$ vs n^{-1}.

The same antisymmetry applies to other pairs separated by an odd number of lattice bonds, whereas those separated by an even number correspond to symmetric functions $\Gamma^{(\nu)}(\lambda)$.

The lowest-order term in $\Gamma^{(1)}(\lambda)$ is linear in λ, and arises from the numerator graph which directly links the nearest-neighbor pair. No terms proportional to λ^3 are present, but paths of five steps (going the long way around hexagons including the pair) are present, and generate λ^5 contributions. In succeeding odd orders it is necessary to account not only for simple paths connecting the neighbors, but also for paths with pendant polygons, disconnected graphs, and the cancellation of terms (in given λ order) with positive powers of N between numerator and denominator. Lists of polygons utilized in the W_N calculation proved useful in generating the simple paths, merely by excising one side at a time from each, and noting whether the preceding and succeeding sides were parallel or not.

The $\Gamma^{(1)}$ power series, through 13th order, is found to be

$$\Gamma^{(1)}(\lambda)=(\lambda/3)-2(\lambda/3)^5-10(\lambda/3)^7-12(\lambda/3)^9 -154(\lambda/3)^{11}-1020(\lambda/3)^{13}-\cdots. \quad (3.6)$$

In order to calculate the series coefficients for the second-neighbor correlation function $\Gamma^{(2)}(\lambda)$, it is necessary to account for the same general types of terms that contribute to $\Gamma^{(1)}(\lambda)$. However, the enumeration of simple paths is somewhat more difficult than before since only a subset may be obtained by removing a pair of contiguous sides from listed polygons. We were

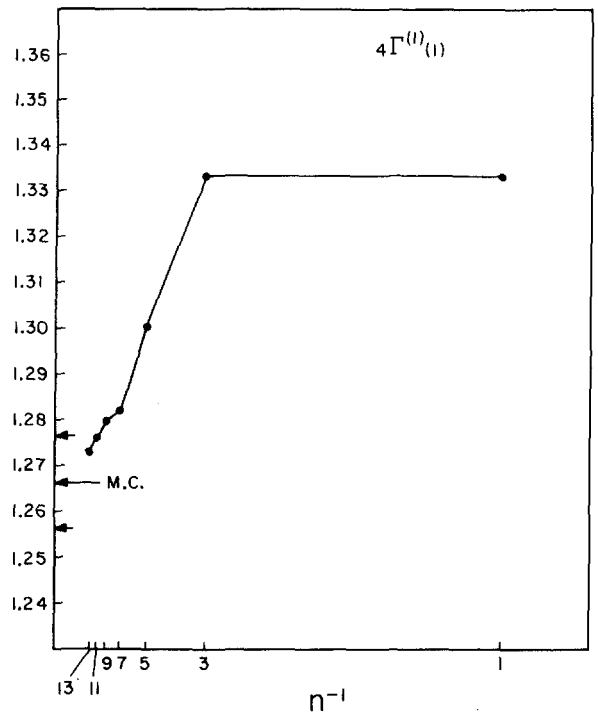

FIG. 4. Partial sums for $4\Gamma^{(1)}(+1)$ vs n^{-1}. The Monte Carlo estimate from Ref. 21 (corrected for finite system effects) is shown by the arrow marked "M.C.," with estimated errors indicated by the small flanking arrows.

nevertheless able to compute the power series coefficients explicitly through 12th order:

$$\Gamma^{(2)}(\lambda)=(1/3)(\lambda/3)^2-2(\lambda/3)^4-4(\lambda/3)^6-6(\lambda/3)^8 -102(\lambda/3)^{10}-(1190/3)(\lambda/3)^{12}-\cdots. \quad (3.7)$$

It has been our experience that the work involved in generating series of given length for the $\Gamma^{(\nu)}$ increases with increasing separation of the pair. For that reason it has not been possible to produce very extensive results for higher-order neighbors. But at least the beginning of the third-neighbor series can be shown:

$$\Gamma^{(3)}(\lambda)=-(2/3)(\lambda/3)^3-(4/3)(\lambda/3)^5-(14/3)(\lambda/3)^7 -34(\lambda/3)^9-\cdots. \quad (3.8)$$

This set of terms reinforces the consistent trend established in Eqs. (3.6) and (3.7): The leading term is always corrected downward by a series of uniformly negative succeeding terms.[26]

The $\Gamma^{(\nu)}$ power series can ultimately be assembled to form the $g_K(\lambda)$ series. If (as before) m_ν denotes the number of neighbors of type ν for a fixed site,[27] then

$$g_K(\lambda)=1+\sum_{\nu=1}^{\infty} m_\nu\Gamma^{(\nu)}(\lambda) \equiv \sum_{n=0}^{\infty} g_{K,n}\lambda^n. \quad (3.9)$$

The coefficients $g_{K,n}$ may be read off of expression (1.6) for $g_K(+1)$. In deriving that expression, Gobush and Hoeve[8] were able to use graph-counting simplifications that are similar to those that were developed for the Ising model,[28] but which unfortunately do not apply to the individual functions $\Gamma^{(\nu)}(\lambda)$.

IV. ANALYSIS OF SERIES

Suppose that the function $F(\lambda)$ is known to be analytic at $\lambda=0$ in the complex λ plane. The radius of convergence R of its power series

$$F(\lambda)=\sum_{n=0}^{\infty} F_n\lambda^n \quad (4.1)$$

is given by the ratio test[29]:

$$R=\lim_{n\to\infty}|F_n/F_{n+1}|, \quad (4.2)$$

provided this limit exists. As $n\to\infty$ therefore,

$$\ln|F_n\lambda^n|\sim A+n\ln|\lambda/R|, \quad (4.3)$$

where A is a suitable constant. In other words the magnitudes of the separate terms in Eq. (4.1), when λ is within the convergence circle, go to zero exponentially fast with increasing order n.

A similar situation applies to the sequence of partial sums S_n for F:

$$S_n(\lambda)=\sum_{j=0}^{n} F_j\lambda^j. \quad (4.4)$$

If the coefficients F_j are real, and beyond some order $n_0\geq 0$ are uniform in sign, then for real positive λ:

$$F(\lambda)-S_n(\lambda)=\sum_{j=n+1}^{\infty} F_j\lambda^j \cong \sum_{j=n+1}^{\infty} A'\exp[j\ln|\lambda/R|+0(n)], \quad (4.5)$$

where A' is another constant. When λ is within the convergence circle, the individual terms in the sum (4.5) decrease exponentially fast with increasing j, so the sum itself therefore must also decrease exponentially fast with n. Consequently, if one were to plot the partial sums $S_n(\lambda)$ vs n^{-1}, with fixed $0<\lambda<R$, the points should lie along an asymptotic curve of extreme flatness at the origin. Plotted in this way, the asymptotic behavior of the partial sums is controlled by the factor

$$\exp[-A''/n^{-1}], \quad (4.6)$$

which, as a function of the continuous variable n^{-1}, has all finite order derivatives at 0+ equal to zero.

Figure 3 displays partial sums, vs n^{-1}, for $4\Gamma^{(1)}(\lambda)$ evaluated at $\lambda=0.5$. There seems to be little doubt that the points shown (for $n\leq 13$) have begun to describe a curve which would eventually intersect the horizontal axis with zero slope and zero curvature. Whether or not higher derivatives would also vanish cannot be determined for sure, but it seems quite safe

tentatively to suppose that $\lambda=0.5$ is well within the circle of convergence.

The quantity which is relevant to the Kirkwood factor $g_K(+1)$ is $4\Gamma^{(1)}(+1)$. The corresponding partial sums vs n^{-1} which appear in Fig. 4 convey quite a different picture. Approach to the $n\to\infty$ limit would appear to be roughly linear (i.e., along a straight line with positive slope). The result for $4\Gamma^{(1)}(+1)$ from the Monte Carlo calculation of Ref. 21 has also been included in Fig. 4, and within its estimated error seems to agree with the intercept of a linear extrapolation for the partial sums.

The contribution of the 12 equivalent second neighbors to $g_K(+1)$ is $12\Gamma^{(2)}(+1)$. The corresponding partial sums (for $n\leq 12$) appear in Fig. 5, along with the Monte Carlo estimate from Ref. 21. Again it seems that the limiting behavior involves a curve with positive slope, whose intercept is in substantial agreement with the Monte Carlo value.

The third neighbor quantity $12\Gamma^{(3)}(+1)$ receives the same treatment in Fig. 6. The trend is less impressive now on account of the foreshortened series, but at least it is plausible that the same positive-slope approach to a limit (in rough agreement with the Monte Carlo calculation) applies.

The collective implication generated by Figs. 4, 5, and 6 is that $\lambda=+1$ is *on* the convergence circle for perturbation theory of the correlation functions. In fact, the apparent ultimate sign uniformity of the $\Gamma^{(p)}$ series coefficients heralds the existence of a singularity *at* the point $\lambda=+1$. That this point is singular perhaps should not be too surprising, since as noted earlier it corresponds to $\beta w\to+\infty$.

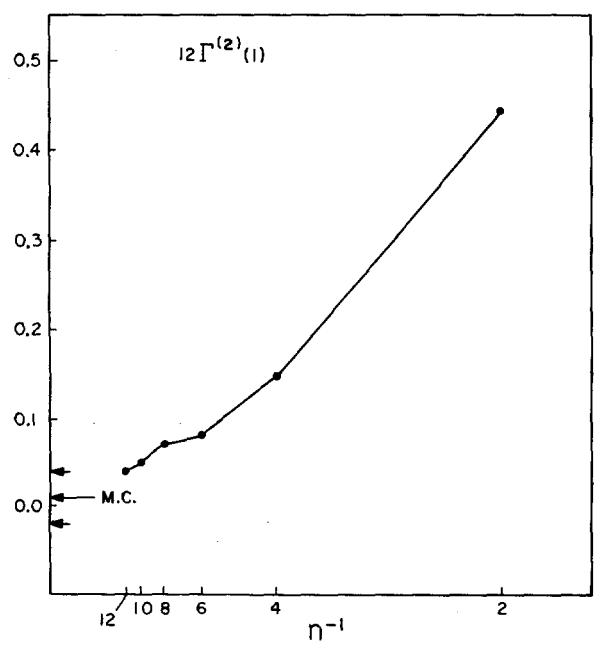

FIG. 5. Partial sums for $12\Gamma^{(2)}(+1)$ vs n^{-1}. The arrows indicate Monte Carlo results from Ref. 21.

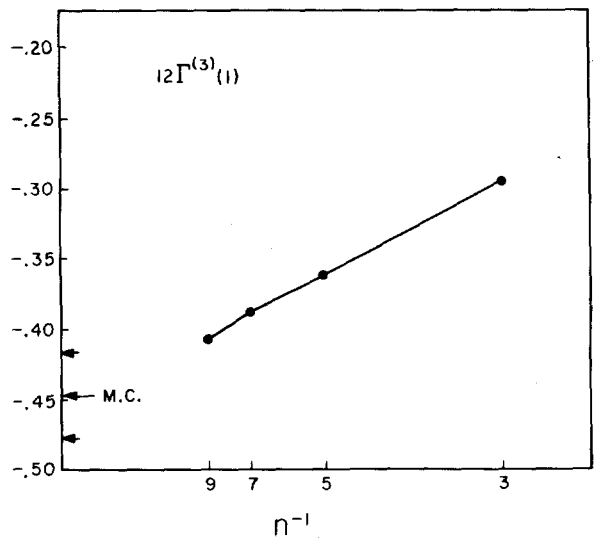

FIG. 6. Partial sums for $12\Gamma^{(3)}(+1)$ vs n^{-1}. Monte Carlo results from Ref. 21 are shown by arrows.

Other independent evidence tending to support the existence of a singularity at $\lambda=+1$ can also be cited. The configurational states of occupation of the cubic and hexagonal ice lattices may trivially be regarded as permissible arrangements of rigid bent trimers on the lattice: The centers of the boomerang-shaped trimers occupy oxygen sites, and the arms use up one bond apiece. It is then important to recall that an analogous problem—the filling of a square lattice by rigid dimers—leads to orientational correlations that decay only algebraically with increasing pair distance, not exponentially.[30] Evidently particle rigidity forces local order to propagate farther than it would in the presence of occasional overlaps. It seems unlikely that, on the one hand, this situation could obtain for rigid dimers in two dimensions while on the other hand not obtain for rigid trimers in three dimensions.

The existence of long-range correlations raises the analog to critical phenomena. In the case of the Ising model, the role of our coupling constant λ is played by the quantity[31]

$$\Lambda=\tanh(\beta J), \tag{4.7}$$

where $-J$ is the nearest-neighbor interaction. There, as Λ increases from zero (i.e., as temperature declines from infinity toward the critical temperature), the range of correlation increases until its exponential decay constant (inverse correlation length) vanishes. This vanishing, at Λ_c, determines the critical point, and likewise involves algebraic correlation decay.[32] It is well known that correlation functions and thermodynamic properties for the Ising model, as functions of the complex variable Λ, are singular at Λ_c. Thus the configurational problem, and Ising critical points, appear to have common features; nevertheless one must be careful not to assume that corresponding mathe-

matical singularities for the two need to be precisely the same type.

If ice Ic corresponds to the singular limit of perturbation theory, it is natural to assume that ice Ih does as well. It is interesting to note that Villain and Schneider[33] have applied a "random walk approximation" to the study of configuration correlations in ice Ih. Their analysis clearly implies the existence of algebraic correlation tails, as they themselves remark, though perhaps the approximation modifies exponents somewhat compared to the exact values.

Suppose that the series coefficients for $\Gamma^{(\nu)}(\lambda)$ behave asymptotically as

$$-C^{(\nu)}/n^{p} \tag{4.8}$$

for large order n, where $C^{(\nu)}>0$, and $p>1$. Then the error in the corresponding partial sums S_n,

$$\Gamma^{(\nu)}(+1)-S_n(+1)\cong -C^{(\nu)}\sum_{j=n+1}^{\infty} j^{-p}, \tag{4.9}$$

may easily be estimated by replacing the sum by an integral:

$$\Gamma^{(\nu)}(+1)-S_n(+1)\cong -(C^{(\nu)}/pn^{p-1}). \tag{4.10}$$

When the partial sums are then plotted vs n^{-1}, the curve will have a shape near the origin characteristic of the $(p-1)$-power function.

We may write

$$\Gamma^{(\nu)}(\lambda)=\Omega^{(\nu)}(\lambda)-C^{(\nu)}\sum_{j=1}^{\infty} j^{-p}\exp(j\ln\lambda), \tag{4.11}$$

where $\Omega^{(\nu)}$ comprises the effect of deviation of series coefficients from form (4.8), and is relatively unimportant for present purposes. If p is not an integer, we may differentiate (4.11) with respect to $\ln\lambda$ a number of times equal to $[p]$, the integer part of p, to obtain

$$\left(\frac{d}{d\ln\lambda}\right)^{[p]}\Gamma^{(\nu)}(\lambda)\sim -C^{(\nu)}\sum_{j=1}^{\infty} j^{-p+[p]}\exp(j\ln\lambda). \tag{4.12}$$

The sum diverges when $\lambda=1$; for slightly smaller λ the exponential function effectively provides a cutoff for the summation at an upper limit:

$$j\cong 1/|\ln\lambda|. \tag{4.13}$$

Therefore,

$$(d/d\ln\lambda)^{[p]}\Gamma^{(\nu)}(\lambda)\sim -\{C^{(\nu)}/p-[p]\}\,|\ln\lambda|^{-1-[p]+p}, \tag{4.14}$$

and then integrating $[p]$ times we conclude that the singularity in $\Gamma^{(\nu)}(\lambda)$ at $\lambda=+1$ would have as its leading character

$$(1-\lambda)^{[p]}\ln|\lambda|^{-1-[p]+p}\sim(1-\lambda)^{p-1}. \tag{4.15}$$

Thus the partial sum plot yields the relevant exponent directly.

The argument must be slightly modified if p is an integer. In that event we differentiate expression (4.11) $p-1$ times:

$$\left(\frac{d}{d\ln\lambda}\right)^{p-1}\Gamma^{(\nu)}(\lambda)\sim -C^{(\nu)}\sum_{j=1}^{\infty} j^{-1}\exp(j\ln\lambda)$$
$$\sim -C^{(\nu)}\ln[1/|\ln\lambda|]$$
$$\sim +C^{(\nu)}\ln(1-\lambda). \tag{4.16}$$

The principal singular character at $\lambda=+1$ is therefore:

$$(1-\lambda)^{p-1}\ln(1-\lambda). \tag{4.17}$$

If our earlier presumption were correct that partial sums for the $\Gamma^{(\nu)}$, plotted against n^{-1}, led to linear asymptotic curves, then p would have to be 2. That in turn would imply a bounded logarithmic singularity

$$(1-\lambda)\ln(1-\lambda). \tag{4.18}$$

However we should not at present reject the possibility that p deviates slightly from 2, so that $(1-\lambda)^{p-1}$ would stand in place of (4.18).

Granted that the individual $\Gamma^{(\nu)}(\lambda)$ are singular at $\lambda=+1$, it seems hard to avoid the conclusion that $g_K(\lambda)$ will also be singular. Indeed the ratios of successive coefficients in series (1.6) appear to approach dangerously close to the point indicating divergence (though the individual terms remain small). In order to produce a satisfactory degree of convergence in $\Gamma^{(1)}$, it was necessary to go at least a dozen orders beyond the first contributing term. The same situation may well be true for the other $\Gamma^{(\nu)}$, but unfortunately the leading contribution for other types of pairs is displaced to higher order by an amount depending on the pair's separation. It thus becomes especially difficult to produce a good account of correlation at large distance by the straightforward perturbation method.

The failure of series (1.6) to agree with the Monte Carlo estimate for $g_K(+1)$ probably stems from that series' failure to include an avalanche of negative terms from $\Gamma^{(\nu)}$ for large-distance pairs. On the basis of the present work, one would guess that extension of the $g_K(\lambda)$ series (1.6) would eventually produce a sign change for coefficients. If logarithmic singularities of type (4.18) actually apply to each $\Gamma^{(\nu)}$, then if it is continuous $g_K(\lambda)$ would probably pass through a maximum for some real positive λ between 0 and $+1$ and develop a slope of $-\infty$ at $+1$. The foreshortened series (1.6) is simply incapable of indicating that sort of behavior, and would distinctly overestimate $g_K(+1)$. At the present stage, therefore, the Monte Carlo approach seems to be the only reliable way to estimate g_K in ice.

It might be noted in passing that whereas the separate $\Gamma^{(\nu)}$ singularities reinforce one another in g_K at $\lambda=+1$ (due to their common algebraic sign), they also probably cancel to a large degree at $\lambda=-1$. This cancellation results from the differing symmetry of the contributing $\Gamma^{(\nu)}$ (pairs of neighbors are alternatively "even" or "odd" in the crystal). Thus $g_K(\lambda)$ may only be weakly singular at $\lambda=-1$, or not singular at all.

V. DISCUSSION

There are several problem areas in which future effort could improve understanding of ice configurational statistics. Some interesting possibilities are the following.

(A) The Monte Carlo technique in Ref. 21 could be generalized in principle to arbitrary real λ between -1 and $+1$, using the bond energy interpretation (2.2). Not only would this permit calculation of the concentration and distribution of Bjerrum defects for variable λ, but it would provide as well a test of the proposed $g_K(\lambda)$ maximum for positive λ below $+1$.

(B) In view of the available transfer-matrix technique for solving the two-dimensional ice problem,[12,15] it would be instructive to examine the orientational pair correlation functions in that model for finite N. This would allow one to verify on an exactly soluble model the existence of the long-range "N^{-1}" correlation, Eq. (1.14), and to observe if it has any angle dependence.

(C) Like the ices, the aqueous clathrate networks involve fourfold hydrogen-bond coordination.[34] However, pentagons of hydrogen bonds appear in these structures, making division of molecules into two equivalent sublattice sets impossible. The ice, anti-ice transformation therefore has no analog for these structures, so relations such as Eqs. (2.9), (2.10), and (2.11) do not exist. It would be interesting to set up the perturbation theory for dipole–dipole correlations on the clathrate networks, to see how series coefficients (and partial sums) compare for close pairs with those in the ices.

(D) It is still unclear why the Pauling approximation of equal *a priori* weights for all Bernal–Fowler configurations is so successful. Surely the interactions between nearest neighbors would alone favor antiparallel arrangement over parallel arrangements.[35] It would be valuable to undertake a study of the way that longer-range interactions, and many-molecule (nonadditive) interactions manage to undo that energetic bias.

ACKNOWLEDGMENT

The authors are grateful to Professor John F. Nagle for pointing out an enumeration error in the original version of this paper.

* Present address: School of Chemistry, Rutgers University, New Brunswick, N.J. 08903.

[1] J. G. Kirkwood, J. Chem. Phys. **7**, 911 (1939).
[2] D. Eisenberg and W. Kauzmann, *The Structure and Properties of Water* (Oxford U.P., New York, 1969); Chapter 3 contains a detailed description of the structures of the various ice polymorphs.
[3] J. D. Bernal and R.H. Fowler, J. Chem. Phys. **1**, 515 (1933).
[4] The very infrequent violations of the ice rules which produce ionic and Bjerrum defects are important for electrical transport and kinetic behavior, but they are negligible for present purposes. See L. Onsager and M. Dupuis, in *Electrolytes*, edited by B. Pesce (Pergamon, New York, 1962).
[5] L. Pauling, J. Am. Chem. Soc. **57**, 2680 (1935).
[6] J. G. Powles, J. Chem. Phys. **20**, 1302 (1952).
[7] G. T. Hollins, Proc. Phys. Soc. **84**, 1001 (1964).
[8] W. Gobush, Jr. and C. A. J. Hoeve, J. Chem. Phys. **57**, 3416 (1972).
[9] E. A. DiMarzio and F. H. Stillinger, Jr., J. Chem. Phys. **40**, 1577 (1964).
[10] J. F. Nagle, J. Math. Phys. **7**, 1484 (1966).
[11] J. F. Nagle, J. Math. Phys. **9**, 1007 (1968).
[12] E. H. Lieb, Phys. Rev. Lett. **18**, 692 (1967).
[13] E. H. Lieb, Phys. Rev. Lett. **18**, 1046 (1967).
[14] E. H. Lieb, Phys. Rev. Lett. **19**, 108 (1967).
[15] E. H. Lieb, Phys. Rev. **162**, 162 (1967).
[16] B. Sutherland, C. N. Yang, and C. P. Yang, Phys. Rev. Lett. **19**, 588 (1967).
[17] R. J. Baxter, Phys. Rev. Lett. **26**, 832 (1971).
[18] Strictly speaking we should have $N\to\infty$ in Eq. (1.9), outside the summation. But if N is comparable to Avogadro's number, this foreshortened version quantitatively suffices.
[19] It is conceivable that C and C' might depend on direction, but if not, then obviously $C'=2C$.
[20] J. F. Nagle, Proceedings of the International Symposium on the Physics and Chemistry of Ice, Ottawa, 14–18 August 1972 (to be published).
[21] A. Rahman and F. H. Stillinger, J. Chem. Phys. **57**, 4009 (1972).
[22] That real ice contains infrequent Bjerrum defects might for some purposes suggest taking λ very slightly (about 1 part in 10^6) less than $+1$. This refinement is unnecessary in the present investigation (see Ref. 4).
[23] The reversal places a water molecule in that configuration for which its dipole vector has changed sign. In the case of square ice, linear molecules rotate 90°.
[24] Even without periodic boundary conditions, and without equal sublattice populations, we would expect the same conclusion to apply with sufficient accuracy, in a large system, for present purposes.
[25] G. Baker, Advan. Theoret. Phys. **1**, 1 (1965).
[26] Our cursory examination of series for higher-order neighbors has failed to uncover a violation of this trend.
[27] The quantities m_r should not be confused with the numbers of sites in the successive, concentric coordination shells. In the square lattice, for example, pairs with relative separation (3, 4) and (5, 0) have the same distance 5, but are inequivalent.
[28] J. W. Essam and M. F. Sykes, Physica **29**, 378 (1963).
[29] E. T. Whittaker and G. N. Watson, *A Course of Modern Analysis* (Cambridge U. P., Cambridge, London 1952), p. 30.
[30] M. E. Fisher and J. Stephenson, Phys. Rev. **132**, 1411 (1963).
[31] C. Domb, Advan. Phys. **9**, 149 (1960); see specifically Sec. 3.4.1.
[32] M. E. Fisher, Repts. Progr. Phys. **30**, 615 (1967).
[33] J. Villain and J. Schneider, International Symposium on Physics and Chemistry of Ice, Ottawa, 14–18 August 1972 (to be published). See also, J. Villain, Sol. State. Communs. **10**, 967 (1972).
[34] L. Pauling, *The Nature of the Chemical Bond* (Cornell U. P., Ithaca, N.Y., 1960), p. 469.
[35] Quantum mechanical Hartree–Fock calculations for pairs of hydrogen-bonded water molecules suggest that the rotational barrier around the bond axis is about 1 kcal/mole; see, for example: D. Hankins, J. W. Moskowitz, and F. H. Stillinger, J. Chem. Phys. **53**, 4544 (1970).